POLITECNICO DI TORINO
Repository ISTITUZIONALE

Deconfined quantum critical points in fermionic systems with spin-charge separation

Original
Deconfined quantum critical points in fermionic systems with spin-charge separation / Baldelli, N., Montorsi, A., Julià-Farré, S., Lewenstein, M., Rizzi, M., Barbiero, L.. - In: PHYSICAL REVIEW. B. - ISSN 2469-9950. - 113:16(2026), pp. 1-14. [10.1103/shfh-584l]

Availability:
This version is available at: 11583/3010932 since: 2026-05-18T07:00:55Z

Publisher:
American Physical Society - APS

Published
DOI:10.1103/shfh-584l

Terms of use:

This article is made available under terms and conditions as specified in the corresponding bibliographic description in the repository

Publisher copyright
APS postprint/Author's Accepted Manuscript e postprint versione editoriale/Version of Record

This article appeared in PHYSICAL REVIEW. B, 2026, 113, 16, and may be found at ttp://dx.doi.org/10.1103/shfh-584l.
Copyright 2026 American Physical Society

(Article begins on next page)

16 September 2026

Deconfined quantum critical points in fermionic systems with spin-charge separation

Niccolò Baldelli,[1] Arianna Montorsi,[2] Sergi Julià-Farré,[1] Maciej Lewenstein,[1,3] Matteo Rizzi,[4,5] and Luca Barbiero[2]

[1] *ICFO - Institut de Ciències Fotòniques, The Barcelona Institute of Science and Technology, 08860 Castelldefels (Barcelona), Spain*
[2] *Institute for Condensed Matter Physics and Complex Systems, DISAT, Politecnico di Torino, I-10129 Torino, Italy*
[3] *ICREA, Pg. Lluís Companys 23, 08010 Barcelona, Spain*
[4] *Institute for Theoretical Physics, University of Cologne, D-50937 Köln, Germany*
[5] *Forschungszentrum Jülich GmbH, Institute of Quantum Control, Peter Grünberg Institut (PGI-8), 52425 Jülich, Germany*

arXiv:2407.04073v4 [cond-mat.str-el] 9 Sep 2025

Deconfined quantum critical points are intriguing transition points not predicted by the Landau–Ginzburg-Wilson symmetry-breaking paradigm which are usually identified by the appearance of a continuous phase transition between locally ordered phases. Here, we reveal the presence of deconfined quantum critical points with unexplored properties. Contrary to previously known examples, we show that the phenomenon of spin-charge separation peculiar to interacting low dimensional fermions can allow for the appearance of partially gapped deconfined quantum critical points. We first infer this point by performing a field theory analysis of generic one-dimensional fermionic systems in the low energy limit. Subsequently, we derive a microscopic model where phase transitions between different locally ordered phases can take place. Here, by performing a numerical analysis we explicitly derive, among others, the gaps, local order parameters and correlation functions behavior, supporting the presence of partially gapped deconfined quantum critical points. Our results thus provide new interesting insights on the widely investigated topic of quantum phase transitions.

I. INTRODUCTION

The mechanism by which one physical state is transformed into a different one, namely a phase transition, represents one of the most fundamental concepts in several areas of physics [1, 2]. In many cases, phase transitions are realized when an order parameter capturing the properties of a physical state abruptly vanishes, thus signaling the appearance of a phase with new features. This specific mechanism is usually defined as a first order or, equivalently, a discontinuous phase transition [3]. Notably, a large variety of phase transitions displaying different behaviors exist. Paradigmatic examples are for instance the Berezinskii–Kosterlitz–Thouless [4, 5], Ising [6] and, the more exotic, symmetric mass generation [7] phase transitions.

Within this diversity, the Landau–Ginzburg-Wilson symmetry-breaking paradigm [8, 9] rigorously predicts the appearance of discontinuous phase transitions connecting locally ordered (LO) phases with different symmetry properties. However, pioneering analysis proved [10, 11] that it is possible to go beyond this paradigm. In particular, quantum fluctuations can generate second order continuous phase transitions between distinct gapped LO phases. This implies the presence of a gap closing, or equivalently, the simultaneous and continuous vanishing of the two order parameters characterizing the different LO phases, at a single point: the deconfined quantum critical point (DQCP) [12]. As proved for two-dimensional systems [10, 11], here very fascinating phenomena including charge fractionalization and emergent gauge fields can appear. In addition, DQCPs are further characterized by the phenomena of symmetry enrichment, meaning that they exhibit symmetry properties not present in any of the two LO phases they connect. This extraordinary variety of physical effects generated an intense theoretical effort which unveiled DQCPs in two-dimensional spin [13–25] and fermionic [26–29] models, as well as in 3D [30–32], and 1D [32–40] Hamiltonians. Notably, these previous studies all focused on systems where only a gap dictates the properties of phases with different symmetries. As a consequence, the gap closing at the transition point was always associated with fully gapless DQCPs, where all the correlations have algebraic decay. This is completely justified by the fact that, in the large majority of possible LO phases, the gaps capturing different degrees of freedom are always intrinsically related. Importantly, recent analysis [41, 42] based on conformal bootstrap [43] challenged the existence of two dimensional DQCPs, while the same technique seems to confirm their presence in 3D [44]. These analysis thus motivate even more the characterization of DQCPs in 1D where highly accurate analytical and numerical techniques are available. Moreover, exact results have been recently produced [38]. In such a context, fermionic systems deserve special attention. Indeed, many-body fermionic Hamiltonians can host the celebrated phenomenon of spin-charge separation [45–47]. This accounts for the decoupling of spin and charge degrees of freedom which can therefore behave completely independently one from the other. Considering all these aspects, it becomes crucial to understand whether DQCPs can exist in the presence of spin-charge separation, and how this phenomenon may influence their properties.

Here, we tackle this fundamental problem. Crucially, we find that spin-charge separation makes possible the

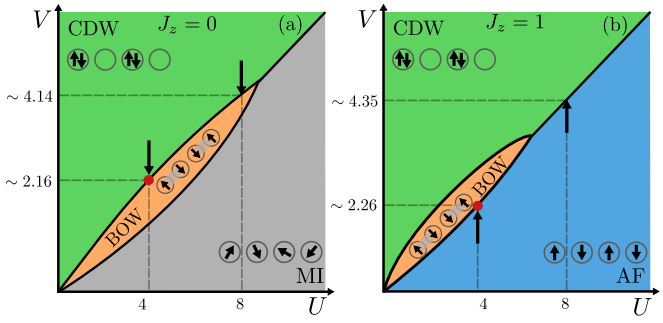

FIG. 1. (a) Cartoon of the phase diagram of the microscopic Hamiltonian in Eq. (17) for $J_z = 0$. The phase diagram consists of a Mott insulator and bond-ordered-wave and a charge density wave. The arrows refer to the transition points studied in section III B 1. (b) Cartoon of the phase diagram of the microscopic Hamiltonian in Eq. (17) for $J_z = 1$. The phase diagram consists of an antiferromagnet and bond-ordered-wave and a charge density wave. The arrows refer to the transition points studied in sections III B 2 and III B 3. In both (a) and (b) the red dots indicate the presence of a partly gapped deconfined quantum critical point.

appearance of a novel kind of DQCPs which, contrary to the previously known examples, have the special feature of being partially gapped. We prove this by considering in section II the sine-Gordon model which well describes generic interacting one dimensional fermions in the low energy limit. By relying on a bosonization analysis [48, 49], we discuss how for conserved total particle number and spin magnetization, three possible fully gapped LO phases can take place: a charge density wave (CDW), an antiferromagnet (AF) and a bond-order-wave (BOW) insulator. Here, bosonization is able to prove the following key aspects: *a)* power law decay of specific correlation functions can occur at the phase transitions between the three different LO phases, thus proving the presence of at least one gap closing in one single point; *b)* in two of these transition points, one gap closes while the other one remains finite as signaled by the long-range behavior of one nonlocal parity correlator; *c)* at each of the three transition points one or two additional continuous symmetries emerge.

In section III we further enforce our findings by deriving a microscopic model where the three LO phases can take place. Here, in addition to bosonization, we perform a Variational Uniform Matrix Product States (VUMPS) [50, 51] based numerical investigation. This method has the advantage that it can directly simulate systems in the thermodynamic limit, allowing for a systematic scaling procedure close to phase transitions [52–54]. In this way, we unveil DQCPs where the concurrent disappearance of two local order parameters are related to the closing of a single gap, either the spin or charge one. Moreover, this analysis rules out a possible second order phase transition where both gaps vanish in one point. In this latter scenario, we indeed observe a first order phase transition as predicted by the Landau theory discuss the previous sentence. On one hand, this result proves the appearance of an emergent $U(1) \times U(1)$ symmetry in the channel associated with the gap closing. On the other, the presence of an additional finite gap induces long-range order of a parity correlator. Moreover, by performing a bond-dimension scaling extrapolation, we accurately extract the critical exponents which govern how the local order parameters vanish at the transition point. Thanks to this analysis, we find values not compatible with the Ising universality class thus supporting the appearance of one dimensional partially gapped DCQPs.

On one hand, our results show that the celebrated phenomenon of spin-charge separation can largely enrich the physical properties of DQCPs and, on the other, our findings provide notable insights towards a deeper understanding of quantum phase transitions.

II. FIELD THEORY OF INTERACTING FERMIONS

A. Derivation of phases with nonlocal or local order

Interacting fermionic systems allow for a field theory description, also called bosonization [48, 49], accurate in the low energy limit. In particular, a generic lattice microscopic Hamiltonian conserving the total magnetization and particles number can be rewritten in the continuum limit as two decoupled sine-Gordon models $\mathcal{H} = \sum_{\nu=c,s} \mathcal{H}_\nu^{SG}$ capturing the spin (s) and charge (c) degrees of freedom

$$\mathcal{H}_\nu^{SG} = \frac{1}{2}\int dx \Big[v_\nu K_\nu (\nabla\vartheta_\nu(x))^2 + \frac{v_\nu}{K_\nu}(\nabla\varphi_\nu(x))^2 + \frac{g_\nu}{\pi^2 a^2}\cos\Big(\sqrt{8\pi}\varphi_\nu(x)\Big)\Big], \tag{1}$$

see Appendix A for more details. Here, v_ν, K_ν and g_ν are the excitation velocities, Luttinger parameters, and coupling amplitudes respectively, which depend on the microscopic Hamiltonian parameters. At the same time, the behavior of the bosonic fields $\varphi_\nu(x)$ and $\vartheta_\nu(x)$ governs the appearance of gapped phases, see A . Specifically, a finite gap Δ_ν in the ν channel develops when $\varphi_\nu(x)$ is pinned to a specific value. Notice that in such a case the effective symmetry relative to the ν channel is $U(1)$ (see Appendix). On the other hand, if $\varphi_\nu(x)$ remains unpinned, the ν channel is gapless and an emergent $U(1) \times U(1)$ [55] symmetry appears. In this regard, eq. (1) provides different solutions describing gapped phases. We start by discussing the following cases: *a)* $\varphi_c = \sqrt{\frac{\pi}{8}}$ and φ_s is unpinned; *b)* $\varphi_s = \sqrt{\frac{\pi}{8}}$ and φ_c is unpinned [56]; *c)* $\varphi_c = \sqrt{\frac{\pi}{8}}$ and $\varphi_s = \sqrt{\frac{\pi}{8}}$. It turns out that gapped phases captured by such specific value $\sqrt{\frac{\pi}{8}}$ of the pinned field $\varphi_\nu(x)$ can be uniquely identified through the nonlo-

	Symmetry Protected Topological Phases			Disordered Phases		Locally Ordered Phases		
	Haldane Insulator	Haldane Liquid	Spin Haldane Insulator	Luther-Emery Liquid	Mott Insulator	Charge Density Wave	Antiferromagnet	Bond Order Wave
Order Parameter	*nonlocal* $\mathcal{O}_S^c$	*nonlocal* $\mathcal{O}_S^s$	*nonlocal* $\mathcal{O}_S^c$, $\mathcal{O}_S^s$	*nonlocal* $\mathcal{O}_P^s$	*nonlocal* $\mathcal{O}_P^c$	*local* $\mathcal{O}_{CDW}$	*local* $\mathcal{O}_{AF}$	*local* $\mathcal{O}_{BOW}$
φ_c	$\sqrt{\pi/8}$	*unpinned*	$\sqrt{\pi/8}$	*unpinned*	0	$\sqrt{\pi/8}$	0	0
φ_s	*unpinned*	$\sqrt{\pi/8}$	$\sqrt{\pi/8}$	0	*unpinned*	0	$\sqrt{\pi/8}$	0
Δ_c	$\neq 0$	0	$\neq 0$	0	$\neq 0$	$\neq 0$	$\neq 0$	$\neq 0$
Δ_s	0	$\neq 0$	$\neq 0$	$\neq 0$	0	$\neq 0$	$\neq 0$	$\neq 0$

TABLE I. List of all the possible gapped phases in one-dimensional fermionic systems with $U(1)$ charge and spin symmetry described by the Hamiltonian in Eq.(1) and derived by studying the microscopic model in Eq.(17). These phases are distinguished by considering the presence of different gaps and their order parameters.

cal string operator

$$O_S^\nu(j) = \mathrm{e}^{i\pi \sum_{i<j} S_i^\nu} S_j^\nu \to O_S^\nu(x) \sim \sin\Big(\sqrt{2\pi}\varphi_\nu(x)\Big) \quad (2)$$

in the microscopic and bosonized version respectively [57, 58], where

$$S_j^s = n_{j\uparrow} - n_{j\downarrow}, \quad S_j^c = 1 - n_j, \quad (3)$$

are fermionic number operators. Here, $n_j = n_{j,\uparrow} + n_{j,\downarrow}$ is the total number of particles. Specifically, states of matter which ordering is captured solely by a finite string order parameter

$$\mathcal{O}_S^\nu = \frac{1}{L}\sum_j \langle O_S^\nu(j)\rangle \to \mathcal{O}_S^\nu \sim \frac{1}{L}\int dx O_S^\nu(x) \quad (4)$$

can be recognized [59] as symmetry protected topological (SPT) phases [60–65]. Based on the formal analogy with the SPT phases occurring in spin-1 Heisenberg [66–68] and Bose-Hubbard models [69–72], the *a)* solution thus describes a charge gapped Haldane insulator. A spin gapped SPT regime also known as Haldane liquid [73, 74] emerges when only $\varphi_s = \sqrt{\frac{\pi}{8}}$ and φ_c keeps fluctuating, i. e. *b)*. Finally, *c)* implies that both $\mathcal{O}_S^\nu \neq 0$ and therefore a fully gapped spin Haldane insulator phase analogous to the topological regime of spinful SSH models [75–78] takes place. Notably, this intrinsic nonlocality makes SPT phases the paradigmatic example of states escaping the Landau's theory of LO states of matter.

Two additional phases characterized by the absence of local order, and therefore also not captured by the Landau's theory, occur when $\varphi_{c(s)} = 0$ and $\varphi_{s(c)}$ is unpinned. Upon defining the nonlocal parity, also called in higher dimension disorder [79–81], operators

$$O_P^\nu(j) = \mathrm{e}^{i\pi \sum_{i<j} S_i^\nu} \to O_P^\nu(x) \sim \cos\Big(\sqrt{2\pi}\varphi_\nu(x)\Big), \quad (5)$$

one can show that their expectation value

$$\mathcal{O}_P^\nu = \frac{1}{L}\sum_j \langle O_P^\nu(j)\rangle \to \mathcal{O}_P^\nu \sim \frac{1}{L}\int dx O_P^\nu(x) \quad (6)$$

represents the order parameters of such phases. More in detail, these two solutions describe: a spin gapped Luther-Emery liquid (LEL) phase where $\varphi_s = 0$ and φ_c is unpinned so that only $\mathcal{O}_P^s \neq 0$; a Mott insulator (MI) where the charge and spin gaps are $\Delta_c \neq 0$, $\Delta_s = 0$, thus reflecting the unpinning of φ_s and the pinning of φ_c to zero so that only $\mathcal{O}_P^c \neq 0$. Because of absence of any local order, we name both LE and MI as disordered phases.

Up to now, the field theory treatment characterized quantum regimes with no local orders. Notably, throughout the above bosonization analysis three fully gapped LO phases can be identified, see Fig. (1) for a cartoon of this regimes. The first one turns out to be a charge density wave (CDW) corresponding to the solution $\varphi_c = \sqrt{\frac{\pi}{8}}$ and $\varphi_s = 0$. Here, the relative local order parameter in his microscopic and bosonized version is represented by a finite expectation value of S_j^c, i.e.

$$\begin{aligned} \mathcal{O}_{CDW} &= \frac{1}{L}\sum_j (-1)^j \langle S_j^c\rangle \to \quad (7)\\ \mathcal{O}_{CDW} &\sim \frac{1}{L}\int dx \langle \sin\Big(\sqrt{2\pi}\varphi_c(x)\Big)\cos\Big(\sqrt{2\pi}\varphi_s(x)\Big)\rangle. \end{aligned}$$

This latter shows the appearance of a LO phase where pairs and empty sites are perfectly alternated thus proving the breaking of the discrete translation symmetry $c_{j\sigma} \to c_{j+1\sigma}$. The second LO regime refers to the solution $\varphi_c = 0$ and $\varphi_s = \sqrt{\frac{\pi}{8}}$. This regime, also known as antiferromagnet (AF), appears when the discrete lattice spin flip invariance $c_{j,\sigma} \to c_{j,-\sigma}$ is broken, reflecting the perfect alternation between fermions with antiparallel spins. In this regard, the local order parameter capturing the AF phase is the expectation value of the staggered magnetization S_j^s

$$\begin{aligned} \mathcal{O}_{AF} &= \frac{1}{L}\sum_j (-1)^j \langle S_j^s\rangle \to \quad (8)\\ \mathcal{O}_{AF} &\sim \frac{1}{L}\int dx \langle \cos\Big(\sqrt{2\pi}\varphi_c(x)\Big)\sin\Big(\sqrt{2\pi}\varphi_s(x)\Big)\rangle \end{aligned}$$

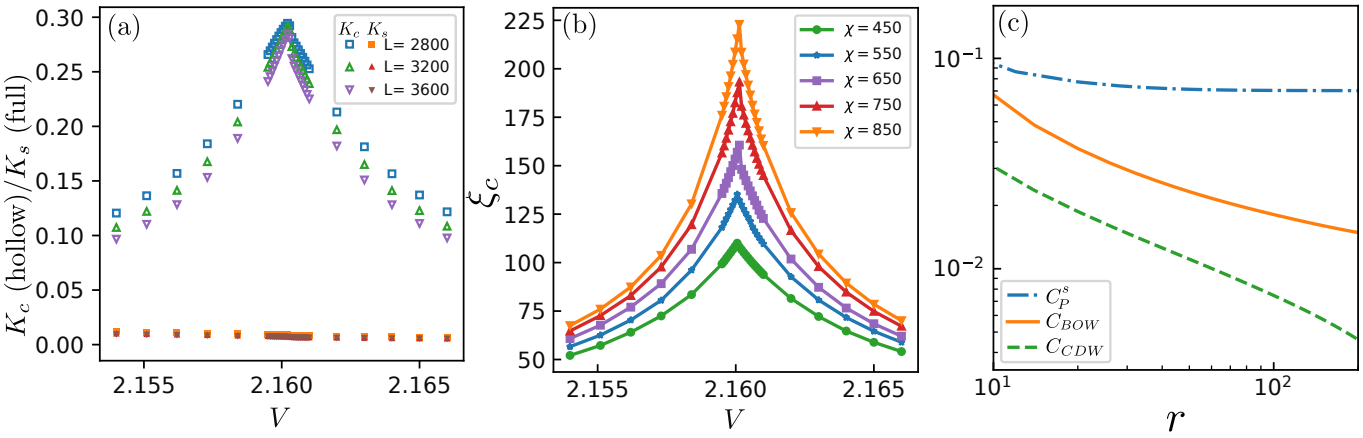

FIG. 2. Study of the critical point between the BOW and the CDW phases appearing in Eq. (17) for $U = 4$, $J_z = 0$ and $t = 1$. (a) Luttinger parameters K_s and K_c. While the first is almost vanishing for all the considered values of V thus proving that the spin gap remains always finite, K_c shows a size independent cusp in one single point thus proving the charge gap closing. Results expressed as a function of a finite MPS of size L, constructed out of $L/2$ unit cells of the infinite MPS. (b) The correlation length ξ_c shows a bond-dimension χ-divergence in the form of a cusp only in one point, also signaling a closing of a gap. (c) Algebraic decay of C_{CDW} and C_{BOW} associated to the long-range order of the spin parity operator correlation C_P^s at the CDW-BOW transition point. All the results have been obtained through VUMPS simulation by keeping a unit cell of two sites.

in its microscopic and bosonized version, respectively. Finally, bosonization predicts an additional LO phase when $\varphi_c = 0$ and $\varphi_s = 0$. This latter, usually called bond-order-wave (BOW) phase, appears when the the discrete site inversion symmetry is broken. As a consequence, an effective lattice dimerization is captured by the local order parameter

$$\mathcal{O}_{BOW} = \frac{1}{L}\sum_j (-1)^j \langle B_j \rangle \to \tag{9}$$
$$\mathcal{O}_{BOW} \sim \frac{1}{L}\int dx \langle \cos\left(\sqrt{2\pi}\varphi_c(x)\right) \cos\left(\sqrt{2\pi}\varphi_s(x)\right)\rangle$$

with $B_j = \sum_\sigma (c^\dagger_{j,\sigma} c_{j+1,\sigma} + h.c.)$.

The complete classification of gapped and partly gapped many-body phases is reported in Table I

B. Beyond Landau phase transitions

The previous analysis allowed us to define three LO regimes. It appears thus crucial to understand whether such phases can be connected through continuous or first order phase transitions. As already pointed out, in the former case the gap vanishes uniquely in one specific point and therefore algebraic decay of the two correlation functions having long-range or exponential decay in the two LO regimes should be predicted. In addition, one should distinguish the case where at these transitions only one of the two gaps closes and reopens from the case where both gaps vanish independently. While this latter scenario might occur at the AF-CDW transition as signaled by the different value of both φ_s and φ_c in AF and CDW, the constant value of $\varphi_s(\varphi_c)$ in BOW and CDW (AF) is compatible with the fact that only $\Delta_c(\Delta_s) = 0$ at the BOW-CDW (AF) transition point. As a consequence, in this last case the presence of a second order transition will be further enriched by one gap $\Delta_\nu \neq 0$ and the corresponding nonlocal order parameter $\mathcal{O}_P^\nu$ will remain finite. Therefore, one might detect a LEL (MI) with spin (charge) parity order at the BOW-CDW (AF). Whereas, in presence of second order AF-CDW transition both gaps have to close and a Luttinger liquid (LL) behavior can take place. Only in this latter case all correlation functions would then display algebraic decay.

In order to better exploit this crucial point, it is convenient to first relate the decay of correlation functions at the transition points to the Luttinger parameters K_ν. In this regards, see A for more details, bosonization shows $K_\nu \approx 0$ in presence of $\Delta_\nu \neq 0$ while K_ν remains thermodynamically finite in presence of a vanishing gap in the ν channel. This point is quite important as the Tomonaga Luttinger theory [45, 46] predicts the K_ν's to induce in the MI, LEL, and LL phases different algebraic decay of the correlation functions $C_X(r)$ (with $X = CDW, AF, BOW$) having long-range order in the X LO phase. Notably, these latter can have the same decay only in a fully gapless Luttinger liquid

$$C_{AF}(r) \sim C_{BOW}(r) \sim C_{CDW}(r) \sim r^{-(K_c+K_s)}. \tag{10}$$

As already discussed, this is the scenario potentially characterizing the AF-CDW phase transition. As a consequence, the expression in Eq. (10) suggests the continuous nature of this phase transition which therefore would be not captured by the Landau's theory. Moreover, bosonization finds that at the BOW-CDW transition solely $K_s = 0$ and therefore the relation showing the

presence of algebraic decay

$$C_{CDW}(r) \sim r^{-K_c} \sim C_{BOW}(r) \tag{11}$$

holds. In addition, the fixed value $\varphi_s = 0$ suggests that long-range order of the spin parity correlation $C^s_P(r) = \langle O^{s\dagger}_P(x) O^s_P(x+r)\rangle$ has to occur. Analogously, at the BOW-AF transition $K_c = 0$, therefore

$$C_{AF}(r) \sim r^{-K_s} \sim C_{BOW}(r) \tag{12}$$

and, in addition, $\varphi_c = 0$ so that $C^c_P(r) = \langle O^{c\dagger}_P(x) O^c_P(x+r)\rangle$ is long-range ordered. The above results clearly point in the direction that exotic partially gapped DQCPs characterized by long-range order of nonlocal order parameter can exist at the BOW-CDW and BOW-AF transition while standard fully gapless DQCPs might appear at the CDW-AF critical point.

III. MICROSCOPIC HAMILTONIAN

As the field theory analysis show evidences of possible very peculiar beyond-Landau phase transitions occurring in strongly interacting fermionic systems, we turn to confirming this intuition at a microscopical level. To do that, we design a lattice Hamiltonian where both the three LO regimes and phase transition between them can occur, see Fig. (1). In particular, while broken translational symmetry is usually induced by the intersite density-density interaction

$$H_{IS}(j) = S^c_j S^c_{j+1}, \tag{13}$$

antiferromagnetic order can emerge in presence of the magnetic coupling

$$H_{AF}(j) = S^s_j S^s_{j+1}. \tag{14}$$

Here, the operators S^c_j and S^s_j are the ones defined in Eq.(3). In addition, the competition between intersite and onsite interaction of the form of

$$H_{OS}(j) = n_{j\uparrow} n_{j,\downarrow} \tag{15}$$

can give rise to BOW ordering [82]. Finally, away from strongly interacting perturbative regimes, quantum fluctuations are induced by tunneling process

$$H_{TP}(j) = \sum_\sigma (c^\dagger_{j,\sigma} c_{j+1,\sigma} + h.c.). \tag{16}$$

All these contributes and their relative strength are captured by the following Hamiltonian

$$H = \sum_j [-tH_{TP}(j) + VH_{IS}(j) + J_z H_{AF}(j) + UH_{OS}(j)]. \tag{17}$$

Notably, this latter presents strong connections with the Hamiltonians [78, 83–85] under investigations in the context of ultracold atomic systems. As these setups are characterized by an unprecedented level of accuracy and versatility, here we restrict our analysis to the regime of half-filling and vanishing total magnetization, i.e. $\sum_j S^\nu_j = 0$ for both $\nu = c, s$.

A. Bosonization analysis

We can extract important information about possible beyond-Landau phase transitions, by applying the bosonization approach to this microscopic model. As shown in Appendix A, bosonization predicts that the transitions between different LO phases occur independently in the two channels but they are captured by the same line

$$U + 2J_z = 2V \quad . \tag{18}$$

Thus, along such line, a continuous CDW-AF transition is predicted, in principle compatible with a fully gapless DQCP. However, it is a well known fact that when the above analysis is complemented by other results, for instance by level crossing analysis [82], the actual transition lines observed in the two channels split: the BOW-CDW and BOW-AF transitions will occur in the weak coupling region, while they will merge into the CDW-AF transition at intermediate couplings only. If this is the case, in the weakly coupled regime this theory turns out to be compatible with the presence of the partially gapped DQCPs envisaged previously.
At the transition lines Eq. (18), one can show A that $K_c \approx 1 - \frac{2V}{\pi t}$ and $K_s \approx 1 - \frac{2J_z}{\pi t}$, differing from each other for any non-vanishing $V \neq J_z$. These values for the Luttinger parameters will be similar at the CDW-AF, or BOW-AF and BOW-CDW transitions. On the other hand, depending on the actual gap closing, eqs. (10), (11), and (12) predict a completely different dependence on K_ν in the power law decay of correlation functions. Thus we expect that the latter will potentially be valuable indicators of the possible type of DQCP.

B. VUMPS analysis

Since bosonization is believed to provide accurate results in the low energy limit, in the following we employ numerical calculations to explore the possible appearance of DQCPs away from this regime. To unveil this point, we perform a numerical analysis based on the VUMPS technique. Here, the state is described by an infinitely repeating unit cell of tensors defined on the sites of the lattice. The tensors are then variationally optimized with a procedure similar to DMRG [86], by using the rest of the (infinite) system as an environment. Compared to infinite DMRG, VUMPS has the advantage to completely replace the full environment at each step, making its convergence significantly faster. This is crucial especially at critical points, where a larger bond dimension is required to get accurate results. Moreover, the absence of boundaries in the variational state makes it easier to escape metastable states that can become more favourable around the critical points in study, where two states that break different symmetries have comparable energies. Indeed, the use of VUMPS has proved critical in the analysis of DQCPs in other systems [34, 39].

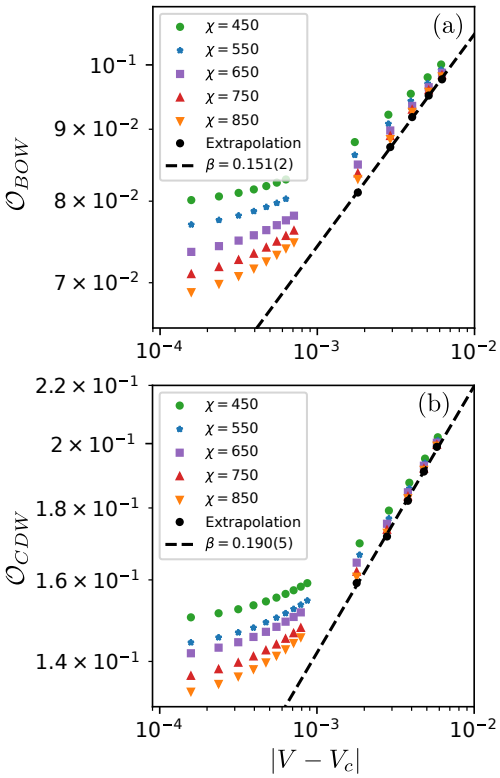

FIG. 3. Scaling of the order parameters around the BOW-CDW transition relative to the model in Eq. (17) for $U = 4$, $J_z = 0$ and $t = 1$ as a function of the bond dimension χ. Both the (a) BOW and the (b) CDW order parameters vanish continuously at transition. By extrapolating the limit $\chi \to \infty$, it is possible to extract the critical exponents $\beta_{CDW}, \beta_{BOW} \neq 1/8$, thus excluding an Ising transition. The details of the extrapolation are detailed in Appendix B

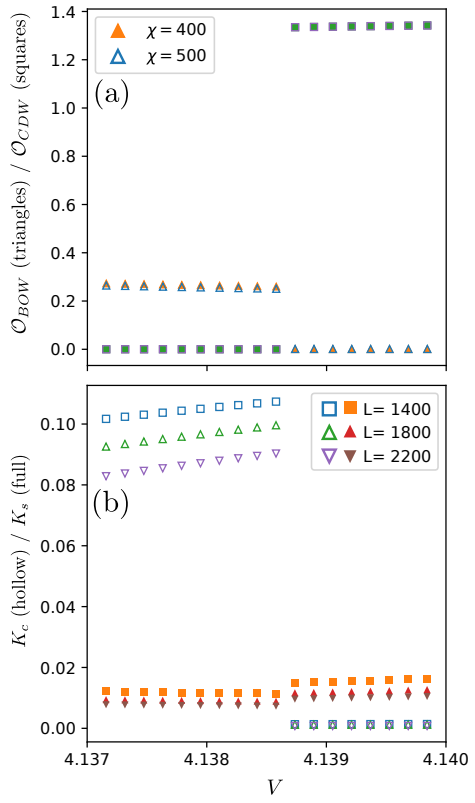

FIG. 4. First order phase transition between the BOW and the CDW phases in the model Eq. (17) for $U = 8, J_z = 0$ and $t = 1$. (a) Values of the order parameters $\mathcal{O}_{BOW}$ and $\mathcal{O}_{CDW}$ for different dimension χ; (a) Values of the Luttinger parameter K_c and K_s at fixed bond dimension. The size L refers to a finite MPS constructed out of $L/2$ unit cells.

1. *BOW-CDW phase transition*

As shown in Fig. (1)(a), for $J_z = 0$, the Hamiltonian in Eq.(17) is the known extended Fermi-Hubbard model [82, 87–90]. For dominating U/t, the system is in a MI phase. The situation changes drastically for larger values of V. Here, two LO phases can take place: a BOW phase when $V \sim U$ are away from strongly interacting perturbative regimes, and a CDW for dominant intersite repulsion. To certify that at the BOW-CDW critical point a gap closing occurs and that it only happens in the charge sector, we extrapolate the Luttinger parameters K_ν. Specifically, we extract their thermodynamic value by computing the static structure factors $P_\nu(q) = \frac{1}{L}\sum_r e^{iqr}\langle S^\nu_j S^\nu_{j+r}\rangle$ which relate to the Luttinger constants through the equation

$$K_\nu = \lim_{q\to 0}\frac{P_\nu(q)}{q} \sim 2\pi \lim_{L\to\infty}\frac{P_\nu(q = 2\pi/L) - P_\nu(q = 0)}{L}. \tag{19}$$

As discussed in the previous sections, this quantity is expected to be zero for a finite Δ_ν, and finite in the case of a gapless ν-channel. To perform the finite-size scaling, we construct multiple finite MPS of length L by repeating $L/2$ unit cells obtained from the VUMPS optimization. Although our analysis considers relatively large interactions $U/t = 4$, our VUMPS simulations provide results compatible with the field theory. On one hand, in Fig.2(a) we indeed find that $K_s \approx 0$ at the CDW-BOW transition point, meaning that $\Delta_s \neq 0$. On the other, K_c shows a L-dependence compatible with a vanishing thermodynamic value for all the considered values of V, except at the transition point where the size dependence is absent. This strongly points in the direction that a continuous phase transition between the two LO regimes persists not only in the low energy limit. In order to enforce this aspect, we extract the correlation length $\xi_\nu(\chi)$ relative to the ν degrees of freedom [91]. A genuine second-order phase transition can indeed be identified by considering the scaling of the correlation length ξ_ν as a function of the bond dimension χ. In particular, one has to expect that in presence of a single point gap closing, the correlation length would show a χ-dependence in the form of a cusp uniquely at that point. Fig. 2(b) shows this behavior for ξ_c, thus strongly supporting the continuous nature of this transition. Notably, this charge gap closing clearly supports the phenomenon of symme-

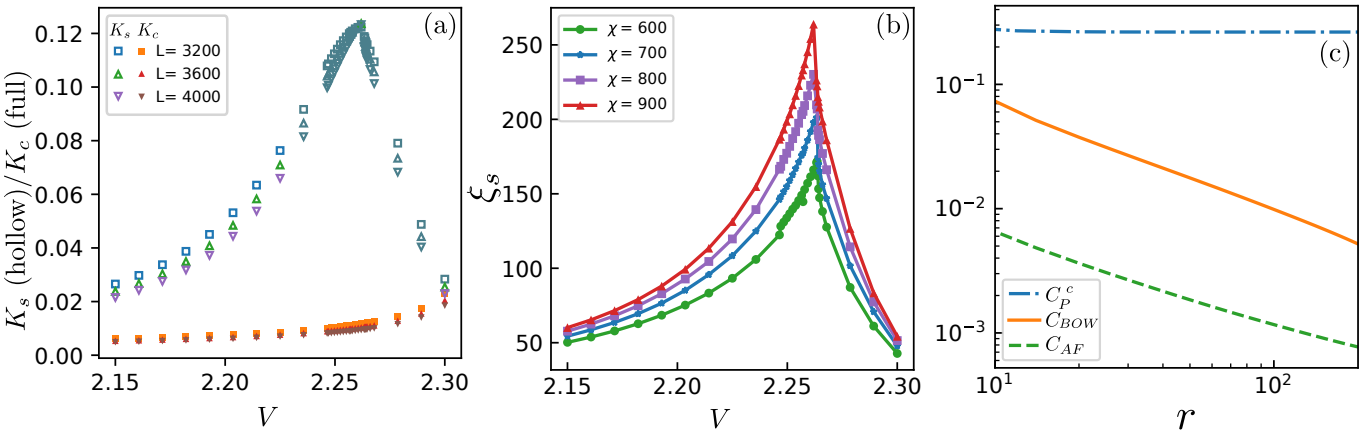

FIG. 5. Study of the critical point between the BOW and the AF phases appearing in Eq. (17) for $U = 4$, $J_z = t = 1$. (a) Luttinger parameters K_c and K_s. While the first is almost vanishing for all the considered values of V thus proving that the spin gap remains always finite, K_s shows a size independent cusp in one single point thus proving the spin gap closing. Results expressed as a function of a finite MPS of size L, constructed out of $L/2$ unit cells of the infinite MPS. (b) The correlation length ξ_s shows a bond-dimension χ-divergence in the form of a cusp only in one point, also signaling a closing of a gap. (c) Algebraic decay of C_{AF} and C_{BOW} associated to long-range order of the charge parity correlator C_P^c at the AF-BOW transition point. All the results have been obtained through VUMPS simulation by keeping a unit cell of two sites.

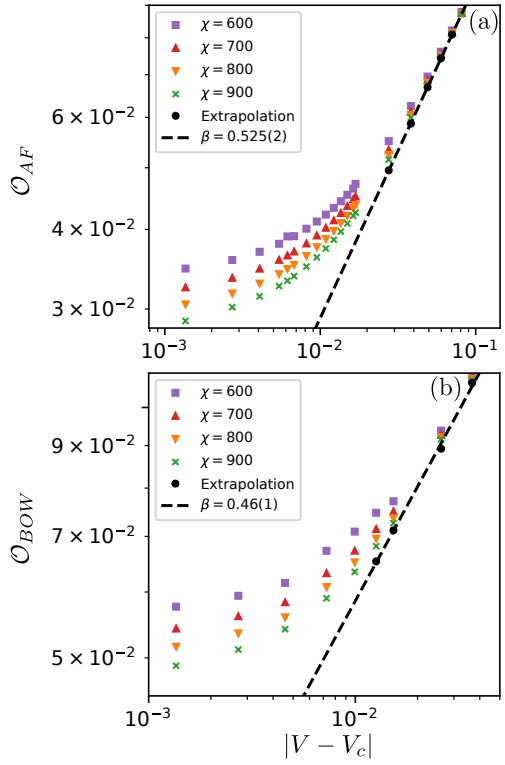

FIG. 6. Scaling of the order parameters around the the AF-BOW transition point in appearing in Eq. (17) for $U = 4$, $J_z = t = 1$ as a function of the bond dimension χ. Both the (a) AF and the (b) BOW order parameters vanish continuously at transition. By extrapolating the limit $\chi \to \infty$, it is possible to extract the critical exponent $\beta_{AF}, \beta_{BOW} \neq 1/8$, excluding an Ising transition.

try enriching. Indeed, based on known symmetry properties of SG model (see Appendix), the presence of a gapless sector is associated to a $U(1) \times U(1)$ (possibly $SU(2)$) symmetry in the same sector. It is straightforward to realize that such emergent symmetry relative to the charge degrees of freedom –not present either in BOW and CDW phases– takes place at the CDW-BOW transition point. Further relevant information can be derived by calculating the decay of the correlators in $C_{CDW}(r)$ and $C_{BOW}(r)$. Fig. 2(c) clearly shows their expected algebraic decay at the transition point. In addition, the same figure confirms that the spin parity parity correlator has long-range order, i.e. $C_P^s(r) \neq 0$ for $r \to \infty$.

Based on this analysis, we have strong indications that peculiar DQCPs can occur in one-dimensional interacting fermionic systems. As underlined, previous examples found indeed fully gapless DQCPs. As a consequence of the phenomenon of spin-charge separation, our analysis shows instead strong evidences on the presence of DQCPs with a finite gap and long-range order of a nonlocal order parameter.

In order to rule out the possibility to ascribe this phase transition in Ising universality class, in Fig. 3 we report an analysis of the behavior of the local order parameters $\mathcal{O}_{CDW}$ and $\mathcal{O}_{BOW}$. Specifically, we are interested in extracting the critical exponent $\beta_{BOW/CDW}$ governing how the local BOW and CDW order parameters vanish at the transition point, i.e.

$$\mathcal{O}_{BOW/CDW}(|V - V_C) \propto |V - V_C|^{\beta_{BOW/CDW}}. \qquad (20)$$

where V_C is the critical value of the intersite interaction where we detect the charge gap closing. Crucially, while an Ising phase transition would formally imply $\beta_{BOW/CDW} = 1/8$, our results based on an extrapolation in the limit $\chi \to \infty$, see B, find different values of such

critical exponent thus proving this phase transition as an example of a 1D DQCP. As pointed out, with respect to previously investigated DQCPs here such beyond Landau's transition points are further associated to a gapped excitation spectrum giving rise to long-range order of the spin parity operator.

Notably, in agreement with previous finite-size studies on the same model [89], we find the BOW-CDW phase transition becomes discontinuous for larger values of the interactions and therefore the partially gapped DQCPs disappear. However, this result is certainly not surprising. When increasing the contact interaction U, the mean-field treatment of the transition associated to negligible quantum fluctuations becomes indeed more accurate and a genuine first-order transition is expected. We prove this point for $U = 8t$. In this case, the order parameters $\mathcal{O}_{BOW}$ and $\mathcal{O}_{CDW}$ exhibit a sharp jump at the critical point independent of the bond dimension χ, see Fig. 4(a), thus discarding the possibility of a single point gap closing. In addition, the Luttinger parameters K_ν reported in Fig. 4(b) show both a clear discontinuity a the transition point and very small size dependent values thus compatible with a thermodynamic vanishing behaviour.

2. *AF-BOW phase transition*

We now move to the analysis of the model in Eq. (17) for $J_z > 0$ which phase diagram is shown in Fig. (1)(b). As specified, a finite antiferromagnetic coupling allows for the breaking of the discrete spin flip symmetry. A part from slightly moving the transition points, we find indeed that the main role played by small J_z is to replace in the Hamiltonian ground state the disordered MI with a locally ordered AF phase. Thanks to this aspect, we can now perform an analysis analogous to the one made in the previous section to investigate whether the AF-BOW transition point can also be classified as a partially gapped DQCP. Here, we focus on intermediate interactions $U/t = 4$ and $J_z/t = 1$ while varying V/t and we again start by exploring the behavior of the Luttinger parameters. Our results in Fig. 5(a) find that at the transition point $K_c \approx 0$ [92] while K_s shows a finite value not affected by different L. This analysis combined with the clear cusp of $\xi_s(\chi)$ shown in Fig. 5(b) demonstrates that the AF-BOW is also a continuous phase transition where the spin gap closes and Δ_c remains finite. Based of the already pointed out symmetry arguments, this results proves the emergence at the critical point of a $U(1)\times U(1)$ symmetry in the spin channel not present in either the BOW or the AF phase. Fig. 5(c) also demonstrates that such symmetry enriched transition point is associated to long-range order of the C_P^c while the correlators C_{AF} and C_{BOW} decay algebraically. Thanks to these findings, we can again infer that the phase transition between the two locally ordered AF and BOW phases is continuous and thus supporting the possible appearance of a partly gapped DQCP. The results in Fig. 6 confirm this intuition. As before, we can indeed show that local order parameters $\mathcal{O}_{AF}$ and $\mathcal{O}_{BOW}$ vanish continuously at the transition point. Moreover, through a χ-extrapolation we calculate their critical exponent

$$\mathcal{O}_{BOW/AF}(|V - V_C) \propto |V - V_C|^{\beta_{BOW/AF}}, \qquad (21)$$

and we find $\beta_{AF} \sim 0.525$ and $\beta_{BOW} \sim 0.46$, again discarding the possibility of an Ising transition. As a consequence, this result proves again that the decoupling between spin and charge degrees of freedom can support the appearance a partly gapped DQCP which in the specific BOW-AF case is characterized by $\Delta_c \neq 0$ while having long-range order of $C_P^c(r)$.

Because of the specific values of the considered J_z, we do not find conclusive evidences of the possible disappearance of these DQCPs for larger interaction where, in analogy with previous case, the BOW-AF transition might become discontinuous. This is because the BOW phase disappears when increasing U before the onset of a first-order BOW-CDW transition could happen. Nevertheless, it cannot be excluded that such a change of behaviour could happen for a different value of J_z.

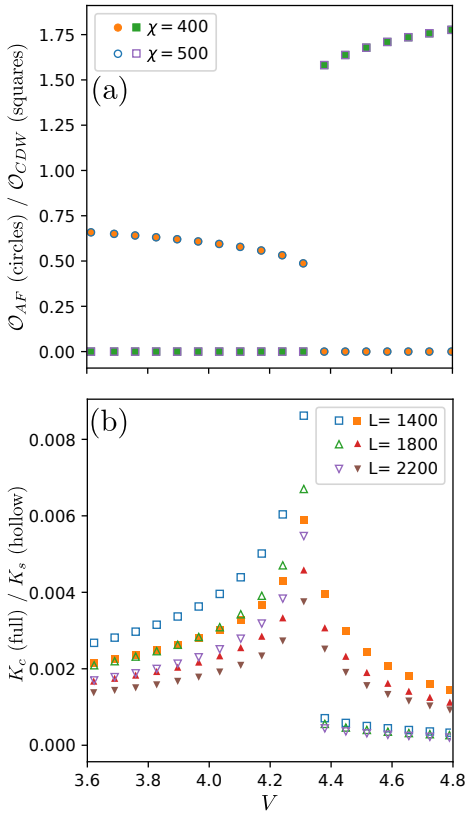

FIG. 7. First order phase transition between the AF and the CDW phases appearing in Eq. (17) for $U = 8$ and $J_z = t = 1$. (a) Values of the order parameters $\mathcal{O}_{BOW}$ and $\mathcal{O}_{AF}$ for different dimension χ; (a) Values of the Luttinger parameter K_c and K_s at fixed bond dimension. The size L refers to a finite MPS constructed out of $L/2$ unit cells.

3. AF-CDW phase transition

Finally, we study the AF-CDW phase transition. As already pointed out at the level of field theory, in order to find such transition to be continuous, both gaps have to vanish at the transition point. This aspect clearly rules out the possible presence of a partly gapped DQCPs while, in principle, it still allows for standard fully gapless DQCPs where all the correlators decay algebraically. As already discussed, the presence of such a DQCPs would require a fine tuning of the microscopic parameters in order to have a simultaneous closing of both the spin and the charge gap. In this regard, our numerical analysis finds that the AF-CDW transition is always first order for all values of U/t. In Fig. 7 we prove this for the case of $U/t = 8$. As can be seen, we find indeed that both the order parameters $\mathcal{O}_{CDW}$ $\mathcal{O}_{AF}$ and the Luttinger parameters display a discontinuity at the transition point, see Fig. 7(a) and (b) respectively. Moreover, while the former quantities are not affected by different χ values, the latter always show size dependence associated to almost vanishing values.

IV. CONCLUSIONS

We unveiled a new type of deconfined quantum critical points. Contrary to previously known examples where they are associated to fully gapless excitations, we have shown that the phenomenon of spin and charge separation can generate partly gapped deconfined quantum critical points. Specifically, by means of analytical and numerical treatments, we have been able to prove that specific phase transitions connecting locally ordered fermionic phases are not captured by the Landau-Ginzburg-Wilson symmetry-breaking paradigm. Notably, at these phase transitions we find that only one gap closes while the other remains finite. Therefore, long-range order of specific nonlocal correlation functions occurs. In addition, we calculated the critical exponents governing how the local order parameters vanish. In such a way, we demonstrated that these transitions are one-dimensional realizations of deconfined quantum critical points with the intriguing feature of being only partly gapped. In conclusion, we also point out that at least one of these phase transitions, the one between the bond-order-wave and charge-density-wave, has been predicted to characterize the phase diagram of ultracold dipolar atoms in optical lattice [78, 93]. Here, the presence of partially gapped deconfined quantum critical points can be probed by measuring the defect production [94–96] predicted by the Kibble-Zurek mechanism [97–102] in continuous transitions. In addition, quantum gas microscopy [103] and noise correlators measurements [104] allow for an accurate detection of local density [105] and spin [106] orderings and therefore for an accurate probing of nonlocal order parameters and locally ordered phases. As consequence, we believe that our results not only unveil a novel interesting type of deconfined quantum critical points but also pave the way towards their experimental detection, which represents a fundamental challenge solid state platforms. [107–110].

ACKNOWLEDGMENTS

We acknowledge useful discussions with M. P. A. Fisher, M. Oshikawa, G. Palumbo and L. Santos. ICFO group acknowledges support from: ERC AdG NOQIA; MCIN/AEI (PGC2018-0910.13039/501100011033, CEX2019-000910-S/10.13039/501100011033, Plan National FIDEUA PID2019-106901GB-I00, Plan National STAMEENA PID2022-139099NB-I00 project funded by MCIN/AEI/10.13039/501100011033 and by the "European Union NextGenerationEU/PRTR" (PRTR-C17.I1), FPI); QUANTERA MAQS PCI2019-111828-2); QUANTERA DYNAMITE PCI2022-132919 (QuantERA II Programme co-funded by European Union's Horizon 2020 program under Grant Agreement No 101017733), Ministry of Economic Affairs and Digital Transformation of the Spanish Government through the QUANTUM ENIA project call – Quantum Spain project, and by the European Union through the Recovery, Transformation, and Resilience Plan – NextGenerationEU within the framework of the Digital Spain 2026 Agenda; Fundació Cellex; Fundació Mir-Puig; Generalitat de Catalunya (European Social Fund FEDER and CERCA program, AGAUR Grant No. 2021 SGR 01452, QuantumCAT U16-011424, co-funded by ERDF Operational Program of Catalonia 2014-2020); Barcelona Supercomputing Center MareNostrum (FI-2023-1-0013); EU Quantum Flagship (PASQuanS2.1, 101113690); EU Horizon 2020 FET-OPEN OPTOlogic (Grant No 899794); EU Horizon Europe Program (Grant Agreement 101080086 — NeQST), ICFO Internal "QuantumGaudi" project; European Union's Horizon 2020 program under the Marie Sklodowska-Curie grant agreement No 847648; "La Caixa" Junior Leaders fellowships, La Caixa" Foundation (ID 100010434): CF/BQ/PR23/11980043. A. M. acknowledges financial support from the ICSC – Centro Nazionale di Ricerca in High Performance Computing, Big Data and Quantum Computing, funded by European Union – NextGenerationEU (Grant number CN00000013). M.R. acknowledges support from the Deutsche Forschungsgemeinschaft (DFG) via project Grant No. 277101999 within the CRC network TR 183 and the EU Quantum Flagship (PASQuanS2.1, 101113690). L. B. acknowledges financial support within the DiQut Grant No. 2022523NA7 funded by European Union – Next Generation EU, PRIN 2022 program (D.D. 104 - 02/02/2022 Ministero dell'Università e della Ricerca). Views and opinions expressed are, however, those of the author(s) only and do not necessarily reflect those of the European Union, European Commission, European Climate, Infrastructure and Environment Executive Agency (CINEA), or any other granting authority.

Neither the European Union nor any granting authority can be held responsible for them.

Appendix A: Field theory approach

The standard field theory treatment of 1D lattice systems of correlated fermions is based on a weak coupling approach, known as bosonization. As this technique has been largely employed, see [48, 49] for exhaustive references, here we just summarize the relevant steps needed to derive the low energy properties of a many-body fermionic system with short range interaction within Abelian bosonization. The starting point consists in defining the continuum limit by replacing the discrete sum over sites j with integrals over the coordinate $x = ja$, i.e. $\sum_j \to \frac{1}{a}\int dx$ with a lattice spacing. Thanks to the peculiar nature of the one dimensional Fermi surface consisting of just two disconnected points $\pm k_F$, usual fermionic operators $c_{j\sigma}, c^\dagger_{j\sigma}$, with $\sigma =\uparrow,\downarrow$ labeling the spin orientation, can be rewritten in terms of right (R) and left (L) fermionic fields $\psi_{\chi\sigma}(x)$ ($\chi = R, L$),

$$c_{j\sigma} \to \sqrt{a}\left[e^{ik_F x}\psi_{R\sigma}(x) + e^{-ik_F x}\psi_{L\sigma}(x)\right] \quad . \tag{A1}$$

The bosonization procedure amounts to rewriting the above fields as appropriate exponentials of bosonic fields $\phi_{\chi\sigma}(x)$, multiplied by a Klein factor $\eta_{\chi\sigma}$ to reproduce their correct anticommutation algebra: $\psi_{\chi\sigma}(x) = \frac{\eta_{\chi\sigma}}{\sqrt{2\pi\alpha}} e^{i\sqrt{4\pi}\chi\phi_{\chi\sigma}(x)}$. It is then customary to introduce first the linear combinations $\phi_\sigma(x) = \phi_{R\sigma}(x) + \phi_{L\sigma}(x)$ and $\theta_\sigma(x) = \phi_{R\sigma}(x) - \phi_{L\sigma}(x)$; and finally their superpositions $\varphi_c(x) = \phi_\uparrow + \phi_\downarrow$, and $\varphi_s(x) = \phi_\uparrow - \phi_\downarrow$, and similarly $\vartheta_c = \theta_\uparrow + \theta_\downarrow$ and $\vartheta_s = \theta_\uparrow - \theta_\downarrow$. At half filling $k_F = \pi/(2a)$ the resulting mapping reads:

$$\psi_{\chi\sigma} = \frac{\eta_{\chi\sigma}}{\sqrt{2\pi\alpha}} e^{i\sqrt{\frac{\pi}{2}}[\chi\varphi_c(x) + \vartheta_c(x) + \sigma(\chi\varphi_s(x) + \vartheta_s(x))]} \quad , \tag{A2}$$

where, with an abuse of notation, χ and σ in the exponent now stand for signs: $R = +$ and $L = -$, $\uparrow = +$ and $\downarrow = -$. Moreover $\alpha \sim a$ is an ultraviolet cutoff, and appropriate commutation relations hold between the bosonic fields. The procedure outlined above allows describing the low energy behavior of most one dimensional fermionic systems. In case of conserved total magnetization and particle number a fermionic system is described by two decoupled sine-Gordon models $\mathcal{H} = \sum_{\nu=c,s} \mathcal{H}^{SG}_\nu$ in the spin (s) and charge (c) degrees of freedom. Explicitly:

$$\mathcal{H}^{SG}_\nu = \frac{1}{2}\int dx \Big[v_\nu K_\nu (\nabla\vartheta_\nu(x))^2 + \frac{v_\nu}{K_\nu}(\nabla\varphi_\nu(x))^2 + \frac{g_\nu}{\pi^2 a^2}\cos\Big(\sqrt{8\pi}\varphi_\nu(x)\Big)\Big] \quad . \tag{A3}$$

Notice that here v_ν, K_ν and g_ν are the excitation velocities, Luttinger parameters, and coupling amplitudes respectively, which depend on the microscopic Hamiltonian parameters. Other cosine terms, which may appear within each sine-Gordon Hamiltonian $\mathcal{H}^{SG}_\nu$ or as coupling terms between the charge and spin sectors, are typically neglected in the low-energy theory. This is because they involve faster oscillations in the bosonic fields and, accordingly, acquire larger scaling dimensions. From a renormalization group (RG) perspective, such terms are therefore irrelevant and do not affect the universal low-energy physics.

1. Derivation of gapped phases and symmetry breaking

In Eq. (A3), the competition between the quadratic and the cosine terms determines the properties of the system. Specifically, in the first line fluctuations of the fields are promoted, whereas the cosine term in the second line favors the pinning of the field $\varphi_\nu(x)$ to a x independent value minimizing the system energy. The resulting phase diagram can be established by means of a well known RG analysis [48] of the model in Eq. (A3). In each channel the cosine term turns out to be irrelevant if the coupling g_ν satisfies

$$2\pi v_\nu(K_\nu - 1) \geq |g_\nu| \quad . \tag{A4}$$

When the cosine term becomes relevant instead, $\varphi_\nu(x)$ prefers to pin to an appropriate constant value, and a gap Δ_ν opens in the corresponding ν-channel. Since the gapless excitations are suppressed, the long wavelength fluctuations and the associated power law behavior of correlations captured by K_ν are also suppressed: K_ν effectively flows to 0 in the ν-channel.

In general, depending on the negative or positive sign of g_ν in Eq. (A4), the pinning values of φ_ν are respectively 0 and $\sqrt{\pi/8}$. In presence of total charge/spin vector conservation of the microscopic lattice Hamiltonian though, the RG flow in the corresponding channel is restricted to solely the line $2\pi v_\nu(K_\nu - 1) = g_\nu$, implying that the cosine term can become relevant only for $g_\nu < 0$ ($\varphi_\nu = 0$). In this case $K_\nu = 1 + \frac{g_\nu}{2\pi v_\nu}$: the theory is gapless for $K_\nu > 1$ and gapped for $K_\nu < 1$. More generally, rooted in the total charge/spin conservation of the lattice Hamiltonian is the global $U(1)$ symmetry

$$\vartheta_\nu \to \vartheta_\nu + const \tag{A5}$$

and a further solution to Eq. (A4) can be found, corresponding to the choice $\varphi_\nu = \sqrt{\pi/8}$ [111].

When the cosine term is irrelevant, the effective Hamiltonian reduces to a Gaussian model, exhibiting the further $U(1)$ symmetry

$$\varphi_\nu(x) \to \varphi_\nu(x) + const \quad , \tag{A6}$$

so that the full symmetry in a gapless channel will be enriched to $U(1) \times U(1) \cong SU(2)$ [112]. When the cosine term becomes relevant though, the above symmetry

becomes discrete, namely

$$\varphi_\nu(x) \to \varphi_\nu(x) + \sqrt{\frac{\pi}{2}} \quad . \tag{A7}$$

Relevantly, also other discrete like the translational, spin-flip and inversion symmetries characterize $\mathcal{H}$, see for instance [32, 82]. According to the Landau's picture [8], some of these could be spontaneously broken generating LO phases captured by a corresponding local order parameter.

2. Bosonization of the microscopic model

The bosonization technique of the microscopic model

$$\begin{aligned} H = & - t\sum_{j,\sigma}(c^\dagger_{j,\sigma}c_{j+1,\sigma} + h.c.) + U\sum_j n_{j,\uparrow}n_{j,\downarrow} \\ & + \sum_j (V S^c_j S^c_{j+1} + J_z S^s_j S^s_{j+1}) \end{aligned} \tag{A8}$$

provides the following quantities

$$\begin{aligned} v_\nu &= 2at(2 - K_\nu), \\ K_c &= 1 - \frac{1}{4\pi t}\big(U + 6V + 2J_z\big), \\ K_s &= 1 - \frac{1}{4\pi t}\big(-U + 2V + 6J_z\big), \\ g_c &= -\big(U - 2V + 2J_z\big)a = -g_s. \end{aligned} \tag{A9}$$

Based on the previous results, it is thus possible to predict that the transitions between LO phases occur independently in the two channels for $g_\nu = 0$. In this case, since $g_c = -g_s$, they identify the same line, namely

$$U + 2J_z = 2V \quad . \tag{A10}$$

Appendix B: Extrapolation of order parameters around criticality

To address the behavior of the order parameters around the DQCPs in Sections III B 1 and III B 2, we have to properly extrapolate their behavior in the limit of infinite bond dimension $\chi \to \infty$. This is crucial as the scaling of these quantities around the critical point leads us to obtain critical exponents incompatible with a transition in the Ising universality class. This, in turn, corroborates our conclusion that we indeed find a DQCP. However, the convergence criterion usually used in VUMPS, only assures that we find a variational minimum in the manifold of the finite bond dimension ansatz in consideration [51]. This does not readily give a measure of the quality of the approximation when compared to the physical ground state.

To overcome this problem we proceed as in standard DMRG, by performing an extrapolation as a function of the discarded Schmidt values after performing a truncation during the optimization process [113].

In particular, to obtain this truncation error, it is sufficient to apply the Hamiltonian H projected on the subspace of the tensors currently being optimized, obtaining a state of bond dimension $d\chi$, where $d = 4$ in the case of spinful fermions. We can then obtain the new ground state in this subspace by performing an exact diagonalization. Finally, by truncating this state back to bond dimension χ we can obtain the error. This procedure is straightforward in the case of two-site DMRG, where the growing of the bond dimension is dynamically performed during the optimization sweep. In the case of VUMPS, however, the bond dimension is kept fixed during the optimization process. We then proceed in the following way: (i) we perform a subspace expansion to express the converged ground state at bond dimension χ using a larger bond dimension 4χ [114]. (ii) We perform one sweep of the VUMPS optimization, equivalent to a single application of H to the unit cell and an exact diag-

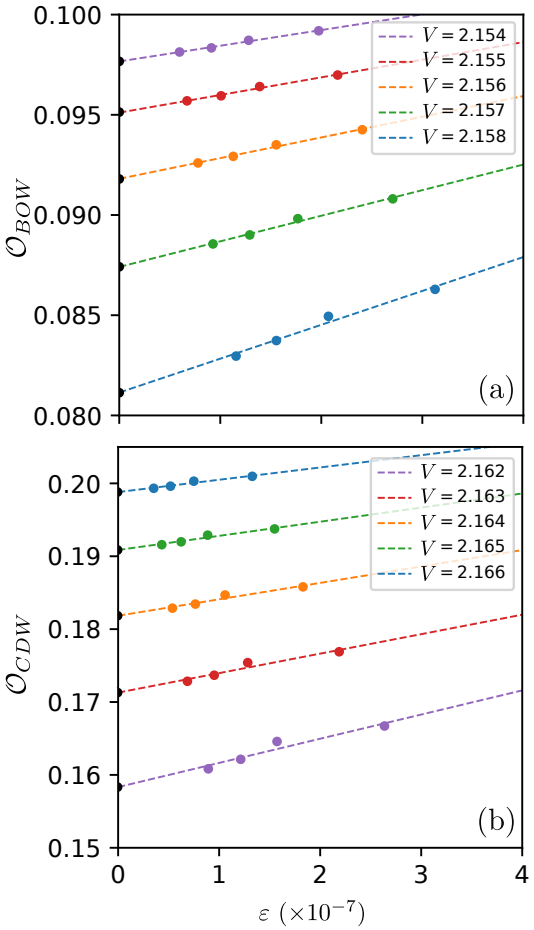

FIG. 8. Extrapolation of the order parameters (a) $\mathcal{O}_{BOW}$ and (b) $\mathcal{O}_{CDW}$, for $\chi \to \infty$, as a function of the density interaction V. We use results computed at $\chi = 550, 650, 750, 850$. The extracted values (black dots) correspond to the extrapolated points in in Fig.3.

onalization in this subspace, (iii) we manually compute the error

$$\varepsilon = \sum_{i=\chi}^{4\chi} S_i^2, \tag{B1}$$

where S_i are the Schmidt values along the bond on which the Hamiltonian is applied. This procedure follows the one explained in Appendix A4 of [51].
In Fig.8 we show, as an example, the value of the order parameters $\mathcal{O}_{BOW/CDW}$ as a function of ε for the BOW-CDW transition showed in Sec. XX. From the extrapolated values of $O_{BOW/CDW}$ we then extracted the critical exponents $\beta_{BOW/CDW}$ by doing a linear fit of the function

$$\begin{aligned} &\log_{10}\left(\mathcal{O}_{BOW/CDW}(V-V_c)\right) = \\ &= \beta_{BOW/CDW}\log_{10}\left(|V-V_c|\right) + \alpha \end{aligned} \tag{B2}$$

using the least squares method. Here, α is a non-universal parameter, not relevant for our analysis. In this way we identified the value of β with an accuracy of the third decimal digit, excluding a value $\beta = 1/8$. We used the same process for the AF-BOW transition to extract the limiting values at criticality of $\mathcal{O}_{AF}$ and $\mathcal{O}_{BOW}$.

[1] C. Domb, M. S. Green, and J. L. Lebowitz, *Phase Transitions and Critical Phenomena*, v.8 (Academic Press, 1972).
[2] S. Sachdev, *Quantum Phase Transitions*, 2nd ed. (Cambridge University Press, 2011).
[3] K. Binder, Theory of first-order phase transitions, Reports on Progress in Physics **50**, 783 (1987).
[4] V. L. Berezinsky, Destruction of long range order in one-dimensional and two-dimensional systems having a continuous symmetry group. I. Classical systems, Sov. Phys. JETP **32**, 493 (1971).
[5] J. M. Kosterlitz and D. J. Thouless, Ordering, metastability and phase transitions in two-dimensional systems, Journal of Physics C: Solid State Physics **6**, 1181 (1973).
[6] L. D. Landau, On the theory of phase transitions, Zh. Eksp. Teor. Fiz. **7**, 19 (1937).
[7] J. Wang and Y.-Z. You, Symmetric mass generation, Symmetry **14** (2022).
[8] L. D. Landau, E. M. Lifshitz, and M. Pitaevskii, *Statistical Physics* (Butterworth-Heinemann, New York, 1999).
[9] K. G. Wilson and J. Kogut, The renormalization group and the ϵ expansion, Phys. Rep. **12**, 75 (1974).
[10] T. Senthil, A. Vishwanath, L. Balents, S. Sachdev, and M. P. A. Fisher, Deconfined quantum critical points, Science **303**, 1490 (2004).
[11] T. Senthil, L. Balents, S. Sachdev, A. Vishwanath, and M. P. A. Fisher, Quantum criticality beyond the landau-ginzburg-wilson paradigm, Phys. Rev. B **70**, 144407 (2004).
[12] T. Senthil, (2023), arXiv:2306.12638 [cond-mat.str-el].
[13] A. W. Sandvik, Evidence for deconfined quantum criticality in a two-dimensional heisenberg model with four-spin interactions, Phys. Rev. Lett. **98**, 227202 (2007).
[14] F.-J. Jiang, M. Nyfeler, S. Chandrasekharan, and U.-J. Wiese, From an antiferromagnet to a valence bond solid: evidence for a first-order phase transition, J. Stat. Mech.: Theory Exp **2008**, P02009 (2008).
[15] J. Lou, A. W. Sandvik, and N. Kawashima, Antiferromagnetic to valence-bond-solid transitions in two-dimensional SU(n) heisenberg models with multispin interactions, Phys. Rev. B **80**, 180414 (2009).
[16] A. Banerjee, K. Damle, and F. Alet, Impurity spin texture at a deconfined quantum critical point, Phys. Rev. B **82**, 155139 (2010).
[17] A. W. Sandvik, Continuous quantum phase transition between an antiferromagnet and a valence-bond solid in two dimensions: Evidence for logarithmic corrections to scaling, Phys. Rev. Lett. **104**, 177201 (2010).
[18] K. Harada, T. Suzuki, T. Okubo, H. Matsuo, J. Lou, H. Watanabe, S. Todo, and N. Kawashima, Possibility of deconfined criticality in su(n) heisenberg models at small n, Phys. Rev. B **88**, 220408 (2013).
[19] K. Chen, Y. Huang, Y. Deng, A. B. Kuklov, N. V. Prokof'ev, and B. V. Svistunov, Deconfined criticality flow in the heisenberg model with ring-exchange interactions, Phys. Rev. Lett. **110**, 185701 (2013).
[20] A. Nahum, J. T. Chalker, P. Serna, M. Ortuño, and A. M. Somoza, Deconfined quantum criticality, scaling violations, and classical loop models, Phys. Rev. X **5**, 041048 (2015).
[21] H. Shao, W. Guo, and A. W. Sandvik, Quantum criticality with two length scales, Science **352**, 213 (2016).
[22] C. Wang, A. Nahum, M. A. Metlitski, C. Xu, and T. Senthil, Deconfined quantum critical points: Symmetries and dualities, Phys. Rev. X **7**, 031051 (2017).
[23] J. Y. Lee, Y.-Z. You, S. Sachdev, and A. Vishwanath, Signatures of a deconfined phase transition on the Shastry-Sutherland lattice: Applications to quantum critical $SrCu_2(BO_3)_2$, Phys. Rev. X **9**, 041037 (2019).
[24] Y.-C. Wang, N. Ma, M. Cheng, and Z. Y. Meng, Scaling of the disorder operator at deconfined quantum criticality, SciPost Phys. **13**, 123 (2022).
[25] M. Song, J. Zhao, L. Janssen, M. M. Scherer, and Z. Y. Meng, (2023), arXiv:2307.02547 [cond-mat.str-el].
[26] Z.-X. Li, S.-K. Jian, and H. Yao, (2019), arXiv:1904.10975 [cond-mat.str-el].
[27] F. F. Assaad and T. Grover, Simple fermionic model of deconfined phases and phase transitions, Phys. Rev. X **6**, 041049 (2016).
[28] Z. H. Liu, W. Jiang, B.-B. Chen, J. Rong, M. Cheng, K. Sun, Z. Y. Meng, and F. F. Assaad, Fermion disorder operator at gross-neveu and deconfined quantum criticalities, Phys. Rev. Lett. **130**, 266501 (2023).
[29] Y. D. Liao, G. Pan, W. Jiang, Y. Qi, and Z. Y. Meng, (2023), arXiv:2302.11742 [cond-mat.str-el].
[30] D. Charrier, F. Alet, and P. Pujol, Gauge theory picture of an ordering transition in a dimer model, Phys. Rev. Lett. **101**, 167205 (2008).

[31] G. J. Sreejith and S. Powell, Scaling dimensions of higher-charge monopoles at deconfined critical points, Phys. Rev. B **92**, 184413 (2015).

[32] C. Mudry, A. Furusaki, T. Morimoto, and T. Hikihara, Quantum phase transitions beyond landau-ginzburg theory in one-dimensional space revisited, Phys. Rev. B **99**, 205153 (2019).

[33] S. Jiang and O. Motrunich, Ising ferromagnet to valence bond solid transition in a one-dimensional spin chain: Analogies to deconfined quantum critical points, Phys. Rev. B **99**, 075103 (2019).

[34] B. Roberts, S. Jiang, and O. I. Motrunich, Deconfined quantum critical point in one dimension, Phys. Rev. B **99**, 165143 (2019).

[35] R.-Z. Huang, D.-C. Lu, Y.-Z. You, Z. Y. Meng, and T. Xiang, Emergent symmetry and conserved current at a one-dimensional incarnation of deconfined quantum critical point, Phys. Rev. B **100**, 125137 (2019).

[36] B. Roberts, S. Jiang, and O. I. Motrunich, One-dimensional model for deconfined criticality with $F_3 \times F_3$ symmetry, Phys. Rev. B **103**, 155143 (2021).

[37] J. Y. Lee, J. Ramette, M. A. Metlitski, V. Vuletić, W. W. Ho, and S. Choi, Landau-forbidden quantum criticality in rydberg quantum simulators, Phys. Rev. Lett. **131**, 083601 (2023).

[38] C. Zhang and M. Levin, Exactly solvable model for a deconfined quantum critical point in 1d, Phys. Rev. Lett. **130**, 026801 (2023).

[39] N. Baldelli, C. R. Cabrera, S. Julià-Farré, M. Aidelsburger, and L. Barbiero, Frustrated extended bose-hubbard model and deconfined quantum critical points with optical lattices at the antimagic wavelength, Phys. Rev. Lett. **132**, 153401 (2024).

[40] A. Romen, S. Birnkammer, and M. Knap, Deconfined quantum criticality in the long-range, anisotropic Heisenberg chain, SciPost Phys. Core **7**, 008 (2024).

[41] Z. Li, Bootstrapping conformal qed3 and deconfined quantum critical point, Journal of High Energy Physics **2022**, 5 (2022).

[42] S. M. Chester and N. Su, Bootstrapping deconfined quantum tricriticality, Phys. Rev. Lett. **132**, 111601 (2024).

[43] D. Poland, S. Rychkov, and A. Vichi, The conformal bootstrap: Theory, numerical techniques, and applications, Rev. Mod. Phys. **91**, 015002 (2019).

[44] S. M. Chester, A. Piazza, M. Reehorst, and N. Su, Bootstrapping the simplest deconfined quantum critical point (2025), arXiv:2507.06283 [hep-th].

[45] S. Tomonaga, Remarks on Bloch's Method of Sound Waves applied to Many-Fermion Problems, Progress of Theoretical Physics **5**, 544 (1950).

[46] J. M. Luttinger, An Exactly Soluble Model of a Many-Fermion System, Journal of Mathematical Physics **4**, 1154 (1963).

[47] F. D. M. Haldane, 'Luttinger liquid theory' of one-dimensional quantum fluids. I. Properties of the Luttinger model and their extension to the general 1D interacting spinless Fermi gas, Journal of Physics C Solid State Physics **14**, 2585 (1981).

[48] A. M. T. Alexander O. Gogolin, Alexander A. Nersesyan, *Bosonization and Strongly Correlated Systems* (Cambridge University Press, 1998).

[49] T. Giamarchi, *Quantum Physics in One Dimension* (Oxford University Press, 2004).

[50] J. Haegeman, T. J. Osborne, and F. Verstraete, Post-matrix product state methods: To tangent space and beyond, Phys. Rev. B **88**, 075133 (2013).

[51] V. Zauner-Stauber, L. Vanderstraeten, M. T. Fishman, F. Verstraete, and J. Haegeman, Variational optimization algorithms for uniform matrix product states, Phys. Rev. B **97**, 045145 (2018).

[52] L. Tagliacozzo, T. R. de Oliveira, S. Iblisdir, and J. I. Latorre, Scaling of entanglement support for matrix product states, Phys. Rev. B **78**, 024410 (2008).

[53] M. M. Rams, P. Czarnik, and L. Cincio, Precise extrapolation of the correlation function asymptotics in uniform tensor network states with application to the bose-hubbard and xxz models, Phys. Rev. X **8**, 041033 (2018).

[54] B. Vanhecke, J. Haegeman, K. Van Acoleyen, L. Vanderstraeten, and F. Verstraete, Scaling hypothesis for matrix product states, Phys. Rev. Lett. **123**, 250604 (2019).

[55] Notice that this may be enhanced to a full $SU(2)$ symmetry in case of symmetric choices of the microscopic parameters of a Hamiltonian[32].

[56] Importantly, this scenario has also been described as a gapless SPT regime [115, 116].

[57] A. Montorsi and M. Roncaglia, Nonlocal order parameters for the 1d hubbard model, Phys. Rev. Lett. **109**, 236404 (2012).

[58] L. Barbiero, A. Montorsi, and M. Roncaglia, How hidden orders generate gaps in one-dimensional fermionic systems, Phys. Rev. B **88**, 035109 (2013).

[59] A. Montorsi, F. Dolcini, R. C. Iotti, and F. Rossi, Symmetry-protected topological phases of one-dimensional interacting fermions with spin-charge separation, Phys. Rev. B **95**, 245108 (2017).

[60] F. Pollmann, E. Berg, A. M. Turner, and M. Oshikawa, Symmetry protection of topological phases in one-dimensional quantum spin systems, Phys. Rev. B **85**, 075125 (2012).

[61] E. Tang and X.-G. Wen, Interacting one-dimensional fermionic symmetry-protected topological phases, Phys. Rev. Lett. **109**, 096403 (2012).

[62] X.-G. Wen, Symmetry-protected topological invariants of symmetry-protected topological phases of interacting bosons and fermions, Phys. Rev. B **89**, 035147 (2014).

[63] Z.-C. Gu and X.-G. Wen, Symmetry-protected topological orders for interacting fermions: Fermionic topological nonlinear σ models and a special group supercohomology theory, Phys. Rev. B **90**, 115141 (2014).

[64] T. Senthil, Symmetry-protected topological phases of quantum matter, Annual Review of Condensed Matter Physics **6**, 299 (2015).

[65] H. Shapourian, K. Shiozaki, and S. Ryu, Many-body topological invariants for fermionic symmetry-protected topological phases, Phys. Rev. Lett. **118**, 216402 (2017).

[66] F. D. M. Haldane, Nonlinear field theory of large-spin heisenberg antiferromagnets: Semiclassically quantized solitons of the one-dimensional easy-axis néel state, Phys. Rev. Lett. **50**, 1153 (1983).

[67] I. Affleck, T. Kennedy, E. H. Lieb, and H. Tasaki, Rigorous results on valence-bond ground states in antiferromagnets, Phys. Rev. Lett. **59**, 799 (1987).

[68] L. Barbiero, L. Dell'Anna, A. Trombettoni, and V. E. Korepin, Haldane topological orders in motzkin spin chains, Phys. Rev. B **96**, 180404 (2017).

[69] E. G. Dalla Torre, E. Berg, and E. Altman, Hidden order in 1d bose insulators, Phys. Rev. Lett. **97**, 260401 (2006).

[70] D. Rossini and R. Fazio, Phase diagram of the extended bose–hubbard model, New Journal of Physics **14**, 065012 (2012).

[71] K. Sugimoto, S. Ejima, F. Lange, and H. Fehske, Quantum phase transitions in the dimerized extended bose-hubbard model, Phys. Rev. A **99**, 012122 (2019).

[72] J. Fraxanet, D. González-Cuadra, T. Pfau, M. Lewenstein, T. Langen, and L. Barbiero, Topological quantum critical points in the extended bose-hubbard model, Phys. Rev. Lett. **128**, 043402 (2022).

[73] S. Fazzini, L. Barbiero, and A. Montorsi, Interaction-induced fractionalization and topological superconductivity in the polar molecules anisotropic $t-j$ model, Phys. Rev. Lett. **122**, 106402 (2019).

[74] A. Montorsi, S. Fazzini, and L. Barbiero, Homogeneous and domain-wall topological haldane conductors with dressed rydberg atoms, Phys. Rev. A **101**, 043618 (2020).

[75] F. Anfuso and A. Rosch, String order and adiabatic continuity of haldane chains and band insulators, Phys. Rev. B **75**, 144420 (2007).

[76] S. R. Manmana, A. M. Essin, R. M. Noack, and V. Gurarie, Topological invariants and interacting one-dimensional fermionic systems, Phys. Rev. B **86**, 205119 (2012).

[77] L. Barbiero, L. Santos, and N. Goldman, Quenched dynamics and spin-charge separation in an interacting topological lattice, Phys. Rev. B **97**, 201115 (2018).

[78] S. Julià-Farré, D. González-Cuadra, A. Patscheider, M. J. Mark, F. Ferlaino, M. Lewenstein, L. Barbiero, and A. Dauphin, Revealing the topological nature of the bond order wave in a strongly correlated quantum system, Phys. Rev. Res. **4**, L032005 (2022).

[79] L. P. Kadanoff and H. Ceva, Determination of an operator algebra for the two-dimensional ising model, Phys. Rev. B **3**, 3918 (1971).

[80] Z. Nussinov and G. Ortiz, Sufficient symmetry conditions for topological quantum order, Proc. Natl. Acad. Sci. U.S.A. **106**, 16944 (2009).

[81] E. Fradkin, Disorder operators and their descendants, Journal of Statistical Physics **167**, 427 (2017).

[82] M. Nakamura, Tricritical behavior in the extended hubbard chains, Phys. Rev. B **61**, 16377 (2000).

[83] E. Guardado-Sanchez, B. M. Spar, P. Schauss, R. Belyansky, J. T. Young, P. Bienias, A. V. Gorshkov, T. Iadecola, and W. S. Bakr, Quench Dynamics of a Fermi Gas with Strong Nonlocal Interactions, Phys. Rev. X **11**, 021036 (2021).

[84] L. Su, A. Douglas, M. Szurek, R. Groth, S. F. Ozturk, A. Krahn, A. H. Hébert, G. A. Phelps, S. Ebadi, S. Dickerson, F. Ferlaino, O. Marković, and M. Greiner, Dipolar quantum solids emerging in a hubbard quantum simulator, Nature **622**, 724 (2023).

[85] A. N. Carroll, H. Hirzler, C. Miller, D. Wellnitz, S. R. Muleady, J. Lin, K. P. Zamarski, R. R. W. Wang, J. L. Bohn, A. M. Rey, and J. Ye, (2024), arXiv:2404.18916 [cond-mat.quant-gas].

[86] S. R. White, Density matrix formulation for quantum renormalization groups, Phys. Rev. Lett. **69**, 2863 (1992).

[87] P. Sengupta, A. W. Sandvik, and D. K. Campbell, Bond-order-wave phase and quantum phase transitions in the one-dimensional extended hubbard model, Phys. Rev. B **65**, 155113 (2002).

[88] A. W. Sandvik, L. Balents, and D. K. Campbell, Ground state phases of the half-filled one-dimensional extended hubbard model, Phys. Rev. Lett. **92**, 236401 (2004).

[89] S. Ejima and S. Nishimoto, Phase Diagram of the One-Dimensional Half-Filled Extended Hubbard Model, Phys. Rev. Lett. **99**, 216403 (2007).

[90] Y. Z. Zhang, Dimerization in a half-filled one-dimensional extended hubbard model, Phys. Rev. Lett. **92**, 246404 (2004).

[91] The correlation length is extracted through the relation $\xi_\nu = -N/\log(\lambda_2)$ where N is the number of sites of a unit cell and λ_2 is second highest eigenvalue of the transfer matrix.

[92] The increasing of K_c for larger values of V/t is due to the fact that the system is approaching the BOW-CDW transition.

[93] M. Di Dio, L. Barbiero, A. Recati, and M. Dalmonte, Spontaneous peierls dimerization and emergent bond order in one-dimensional dipolar gases, Phys. Rev. A **90**, 063608 (2014).

[94] A. Keesling, A. Omran, H. Levine, H. Bernien, H. Pichler, S. Choi, R. Samajdar, S. Schwartz, P. Silvi, S. Sachdev, P. Zoller, M. Endres, M. Greiner, V. Vuletić, and M. D. Lukin, Quantum kibble–zurek mechanism and critical dynamics on a programmable rydberg simulator, Nature **568**, 207 (2019).

[95] N. Xi and R. Yu, Dynamical signatures of the one-dimensional deconfined quantum critical point, Chinese Physics B **31**, 057501 (2022).

[96] Y.-R. Shu, S.-K. Jian, and S. Yin, Nonequilibrium dynamics of deconfined quantum critical point in imaginary time, Phys. Rev. Lett. **128**, 020601 (2022).

[97] T. W. B. Kibble, Topology of cosmic domains and strings, Journal of Physics A: Mathematical and General **9**, 1387 (1976).

[98] T. Kibble, Some implications of a cosmological phase transition, Physics Reports **67**, 183 (1980).

[99] W. H. Zurek, Cosmological experiments in superfluid helium?, Nature **317**, 505 (1985).

[100] W. Zurek, Cosmological experiments in condensed matter systems, Physics Reports **276**, 177 (1996).

[101] A. Polkovnikov, K. Sengupta, A. Silva, and M. Vengalattore, Colloquium: Nonequilibrium dynamics of closed interacting quantum systems, Rev. Mod. Phys. **83**, 863 (2011).

[102] A. del Campo and W. H. Zurek, Universality of phase transition dynamics: Topological defects from symmetry breaking, Int. J. Mod. Phys. A **29**, 1430018 (2014).

[103] C. Gross and W. S. Bakr, Quantum gas microscopy for single atom and spin detection, Nat. Phys. **17**, 1316 (2021).

[104] K. Gallego-Lizarribar, S. Julià-Farré, M. Lewenstein, C. Weitenberg, L. Barbiero, and J. Argüello-Luengo, (2024), arXiv:2404.08374 [cond-mat.quant-gas].

[105] M. Endres, M. Cheneau, T. Fukuhara, C. Weitenberg, P. Schauß, C. Gross, L. Mazza, M. C. Bañuls, L. Pollet, I. Bloch, and S. Kuhr, Observation of correlated particle-hole pairs and string order in low-dimensional mott insulators, Science **334**, 200 (2011).

[106] M. F. Parsons, A. Mazurenko, C. S. Chiu, G. Ji, D. Greif, and M. Greiner, Site-resolved measurement of the spin-correlation function in the fermi-hubbard model, Science **353**, 1253 (2016).

[107] M. E. Zayed, C. Rüegg, J. Larrea J., A. M. Läuchli, C. Panagopoulos, S. S. Saxena, M. Ellerby, D. F. McMorrow, T. Strässle, S. Klotz, G. Hamel, R. A. Sadykov, V. Pomjakushin, M. Boehm, M. Jiménez–Ruiz, A. Schneidewind, E. Pomjakushina, M. Stingaciu, K. Conder, and H. M. Rønnow, 4-spin plaquette singlet state in the Shastry–Sutherland compound SrCu2(BO3)2, Nat. Commun. **13**, 962 (2017).

[108] J. Guo, G. Sun, B. Zhao, L. Wang, W. Hong, V. A. Sidorov, N. Ma, Q. Wu, S. Li, Z. Y. Meng, A. W. Sandvik, and L. Sun, Quantum phases of $srcu_2(bo_3)_2$ from high-pressure thermodynamics, Phys. Rev. Lett. **124**, 206602 (2020).

[109] T. Hong, T. Ying, Q. Huang, S. E. Dissanayake, Y. Qiu, M. M. Turnbull, A. A. Podlesnyak, Y. Wu, H. Cao, Y. Liu, I. Umehara, J. Gouchi, Y. Uwatoko, M. Matsuda, D. A. Tennant, G.-W. Chern, K. P. Schmidt, and S. Wessel, Evidence for pressure induced unconventional quantum criticality in the coupled spin ladder antiferromagnet $C_9H_18N_2CuBr_4$, Nat. Commun. **13**, 3073 (2022).

[110] Y. Cui, L. Liu, H. Lin, K.-H. Wu, W. Hong, X. Liu, C. Li, Z. Hu, N. Xi, S. Li, R. Yu, A. W. Sandvik, and W. Yu, Proximate deconfined quantum critical point in $SrCu_2(BO_3)_2$, Science **380**, 1179 (2023).

[111] Indeed, in this more general case the Luttinger parameters can be written in the form $K_\nu = \frac{1}{2\pi v_\nu}(1 + g_\nu - \kappa_\nu)$, allowing a further solution for $\kappa_\nu > 0$.

[112] Notice that the effective $SU(2)$ symmetry holds in the case of $SU(2)$ symmetric choices of the microscopic parameters of a Hamiltonian.

[113] U. Schollwöck, The density-matrix renormalization group in the age of matrix product states, Ann. Phys. **326**, 96 (2011).

[114] C. Hubig, I. P. McCulloch, U. Schollwöck, and F. A. Wolf, Strictly single-site dmrg algorithm with subspace expansion, Phys. Rev. B **91**, 155115 (2015).

[115] A. Keselman and E. Berg, Gapless symmetry-protected topological phase of fermions in one dimension, Phys. Rev. B **91**, 235309 (2015).

[116] T. Rakovszky, P. Sala, R. Verresen, M. Knap, and F. Pollmann, Statistical localization: From strong fragmentation to strong edge modes, Phys. Rev. B **101**, 125126 (2020).